Energetic-ion excited internal kink modes with weak magnetic shear in $q_0 > 1$ tokamak plasmas*

Wen-Ming Chen(陈文明)[1], Xiao-Gang Wang(王晓钢)[2,†], Xian-Qu Wang(王先驱)[3], and Rui-Bin Zhang(张瑞斌)[1]

[1] State Key Laboratory of Nuclear Physics and Technology, School of Physics, Peking University, Beijing 100871, China
[2] Department of Physics, Harbin Institute of Technology, Harbin 150001, China
[3] Institute of Fusion Science, School of Physical Science and Technology, Southwest Jiaotong University, Chengdu 610031, China

(Received 25 February 2017; revised manuscript received 12 April 2017; published online 10 July 2017)

The energetic particle driven internal kink mode is investigated in this paper for $q_0 > 1$ tokamak plasma with weak magnetic shear. With the effect of energetic particles, the $m/n = 1/1$ internal mode structure in tokamak plasma does not appear as a rigid step-function when safety factor passes through $q = 1$ rational surface. It is found that even when the rational surface is removed, the mode may be still unstable under the low magnetic shear condition if the energetic particle drive is strong enough; with the low shear region of safety factor profile widening, the mode becomes more unstable with its growth-rate increasing. Furthermore, we find that the existence of the $q = 1$ rational surface does not have a significant effect on the stability of the plasma if energetic particles are present, which is very different from the scenarios of the ideal-MHD modes.

Keywords: tokamak instabilities, low magnetic shear, internal kink mode

PACS: 52.30.Cv, 52.35.Py, 52.55.Pi **DOI:** 10.1088/1674-1056/26/8/085201

1. Introduction

Plasma heating and current drive are key issues towards burning plasma.[1] Neutral beam injection (NBI), ion cyclotron resonance heating (ICRH), low hybrid current drive (LHCD), and nuclear fusion reaction not only heat the plasma or drive plasma current efficiently, but also produce a new population of plasma species: energetic particles (EPs).[2–4] The EP physics in fusion plasmas has been investigated extensively due to widely applied auxiliary heating and profile control in recent decades.[5–8] Since the well-known energetic particle mode (EPM), the fishbone mode, was discovered in the Poloidal Divertor eXperiment (PDX) during high-beta operation with NBI, which caused 20%–40% high-energy particles to lose and degraded the efficiency of heating and current drive dramatically,[9] this mode has been substantially investigated theoretically or experimentally, which can be induced by energetic ions and electrons.[10–16] It was shown that the precession of energetic particles destabilizes the internal kink mode[10,11] on the $q = 1$ rational surface under finite shear condition. A spatial separation was assumed that near the rational surface a singular layer was formed with a width on the order of $O(\varepsilon)$; while outside of the singular layer, the radial component of plasma displacement vector was a constant,;.e., $\xi = \text{const.}$ for $r < r_0$, and $\xi = 0$ for $r > r_0$ where r_0 is the radial location of the $q = 1$ rational surface. Inside the layer, a layer equation for the mode displacement was established by variation method in different geometries, and non-ideal effects such as resistivity and finite Larmor radius effect were taken into account.[17,18]

Recently, advanced scenario, with the safety factor profile (q-profile) of low or reversed magnetic shear and q_0 or $q_{\min}$ close to unity, is proposed to get rid of fast and disastrous current driven modes. A spatial separation becomes obscure due to very weak or vanished shear in the vicinity of the rational surface with weak Alfvén continuum damping, and the mode structure is more like an infernal mode structure instead of the rigid kink structure for conventional kink mode.[19] For a reversed magnetic shear configuration induced by off-axis current drive, when $q_{\min} < 1$ a double fishbone mode (DFM) can be observed when using auxiliary heating, whose mode structure is quite different from that of the conventional double kink mode.[20] DFM structure has a non-zero $\mathrm{Im}(\xi)$ due to energetic particle, and its frequency is very close to the half of the precession frequency of energetic particle.[21]

In this paper, we further investigate the effect of diverse current profiles, i.e., different q-profiles, especially in the case of $q_0 > 1$, on the instability caused by energetic particles. Without a clear scale separation, we then use a new approach to self-consistently calculate the mode structure and frequency, by a general dispersion relation [10,22] $D(\boldsymbol{\xi}, \boldsymbol{\xi}*) = W_{\mathrm{MHD}} - \omega^2 K + W_{\mathrm{h}} = 0$ and a variation equation determining mode structure,[19] where W_{MHD} is the perturbed bulk plasma potential energy, $-\omega^2 K$ is the plasma kinetic energy, and W_{h} is the energetic particle potential energy. Results obtained deviate from those from a simple step-function structure, and it is found that even when the core safety factor is greater than

*Project supported by the National Natural Science Foundation of China (Grant No. 11261140326).
†Corresponding author. E-mail: xgwang@hit.edu.cn
© 2017 Chinese Physical Society and IOP Publishing Ltd

unity, it is still an unstable configuration. It should be pointed out that m/n=1/1 internal kink mode is absent when q_0 is significantly away from unity. More details about effects of magnetic shear, energetic particle beta, and the core safety factor on the mode structure and growth-rate are also discussed.

The rest of this paper is organized as follows. An energy integral equation including the energetic particle contribution and a variation equation are introduced in Section 2, to give an iteration solution of mode frequency and structure simultaneously. By applying a series of q-profiles in Section 3, we investigate the effect of profile shape on the mode. Finally, a brief conclusion can be found in Section 4.

2. Model and basic equations

2.1. Model and equations

The linearized momentum equation in a fluid approximation can be written as

$$\rho_{\rm m}\frac{\partial^2}{\partial t^2}\boldsymbol{\xi} = -\frac{1}{c}(\delta\boldsymbol{j}\times\boldsymbol{B}+\boldsymbol{j}\times\delta\boldsymbol{B}) - \nabla\delta P_{\rm c}, \tag{1}$$

where $\boldsymbol{\xi}$ is the fluid displacement vector, the mass density $\rho_{\rm m} = n_{0i}m_i$, with the subscript i denoting the species, and prefix δ is for the perturbed quantity. Meanwhile, the equation of state can be linearly approximated as

$$\delta P_{\rm c} = -\gamma P_0\nabla\cdot\boldsymbol{\xi} - \boldsymbol{\xi}\cdot\nabla P_0,$$

and Ohm's law

$$\delta\boldsymbol{E}_\perp = -\frac{1}{c}\frac{\partial}{\partial t}\boldsymbol{\xi}\times\boldsymbol{B}, \quad \delta\boldsymbol{E}_\parallel = 0,$$

Faraday's law $\delta\boldsymbol{B} = \nabla\times(\boldsymbol{\xi}\times\boldsymbol{B})$ and Ampere's law

$$\delta\boldsymbol{j} = c\frac{\nabla\times\delta\boldsymbol{B}}{4\pi}.$$

These equations form a closed system to determine the properties of instability.

Decomposing fluid displacement vector

$$\boldsymbol{\xi}(\boldsymbol{r},t) = \boldsymbol{\xi}(r)\mathrm{e}^{\mathrm{i}(m\theta-n\zeta-\omega t)},$$

we obtain the energy equation:

$$W_{\rm MHD} - \omega^2 K = 0, \tag{2a}$$

where $W_{\rm MHD}$ is the perturbed bulk plasma potential energy without the surface term[23] and

$$K = \frac{1}{2}\int \mathrm{d}\boldsymbol{x}\rho_{\rm m}\boldsymbol{\xi}\cdot\boldsymbol{\xi}^*$$

is the plasma kinetic energy. Together with Eq. (2a), we obtain the variation equation:

$$\delta(W_{\rm MHD} - \omega^2 K) = 0, \tag{2b}$$

where the variation is done on perturbed fluid displacement vector, and the two equations will give exactly the same solution as Eq. (1).

The plasma is assumed to be incompressible,$\nabla\cdot\boldsymbol{\xi} = 0$, and through the minimization of $W_{\rm MHD}$, one can obtain

$$\xi_\theta = \mathrm{i}\frac{\mathrm{d}}{\mathrm{d}r}(r\xi)$$

and $\xi_\zeta = 0$. Using this trial function one can estimate the perturbed potential energy contributed from energetic ions by a slowing down distribution[10,24,25]

$$\hat{W}_{\rm h} = \int_0^1 \mathrm{d}\hat{r}3n\hat{\beta}_{\rm h}\frac{2\hat{r}^2}{\pi}\frac{\omega}{\omega_{\rm dm}}\ln\left(1-\frac{\omega_{\rm dm}}{\omega}\right)|\xi|^2,$$

which is normalized by $\dfrac{4\pi^2a^2}{2R_0^2}R_0\dfrac{B_0^2}{4\pi}|\xi_r(0)|^2$, and $\xi \equiv \xi_r/\xi_r(0)$, $\hat{r} = r/a$. Also, $\hat{\beta}_{\rm h} = -(R/3a)(1-\kappa_0^2)a\partial\langle\beta_{\rm h}\rangle_\theta/\partial r$ with $\langle\beta_{\rm h}\rangle_\theta$ representing the averaged poloidal fast ion beta, $\omega_{\rm dm} = \omega_{\rm dh}(E = E_{\rm m})$ with $\omega_{\rm dh}$ denoting the precession frequency of the fast ion, and $\kappa_0^2 = (R/2r)(1/\Lambda - 1 + r/R)$ with $\Lambda\sim 1$ for deeply trapped particle.[25]

2.2. Numerical procedure

Assuming a small inverse aspect ratio $a/R_0\sim\varepsilon$, and a low plasma beta $\beta = 8\pi p/B_0^2\sim\varepsilon^2$, together with the contribution from energetic particles, the energy equation and variation equations become

$$\begin{aligned}
&\int_0^1\hat{r}\left(\frac{n}{m}-\frac{1}{q}\right)^2\left(\hat{r}^2|\frac{\mathrm{d}}{\mathrm{d}\hat{r}}\xi|^2+(m^2-1)|\xi|^2\right)\mathrm{d}\hat{r}\\
&-\frac{3\omega(\omega-\omega_*)}{\omega_{\rm A}^2}\int_0^1\hat{r}\left(|\xi|^2+|\frac{\mathrm{d}}{\mathrm{d}\hat{r}}\left(\frac{\hat{r}\xi}{m}\right)|^2\right)\mathrm{d}\hat{r}\\
&+\frac{\omega}{\omega_{\rm dm}}\ln\left(1-\frac{\omega_{\rm dm}}{\omega}\right)\int_0^1 3n\hat{\beta}_{\rm h}\frac{2\hat{r}^2}{\pi}|\xi|^2\mathrm{d}\hat{r} = 0,
\end{aligned}\tag{3}$$

$$\begin{aligned}
&\frac{\mathrm{d}}{\mathrm{d}\hat{r}}\left\{\hat{r}^3\left[\left(\frac{n}{m}-\frac{1}{q}\right)^2+\frac{3\omega(\omega_*-\omega)}{m^2\omega_{\rm A}^2}\right]\frac{\mathrm{d}}{\mathrm{d}\hat{r}}\xi\right\}\\
&+\left(\frac{1}{m^2}-1\right)\frac{3\omega(\omega_*-\omega)}{m^2\omega_{\rm A}^2}\hat{r}\xi+(1-m^2)\left(\frac{n}{m}-\frac{1}{q}\right)^2\hat{r}\xi\\
&=\frac{\omega}{\omega_{\rm dm}}\ln\left(1-\frac{\omega_{\rm dm}}{\omega}\right)3n\hat{\beta}_{\rm h}\frac{2\hat{r}^2}{\pi}\xi,
\end{aligned}\tag{4}$$

where ω_* is diamagnetic frequency which is important when the mode frequency is as low as being able to compare with it.[12] In our case, nevertheless, we assume that the mode frequency is greatly larger than the fast ion diamagnetic frequency, so ω_* can be ignored for simplicity. Moreover, we reasonably set $\omega_{\rm dm}$=0.01$\omega_{\rm A}$. For a specific trial eigenvalue ω, equation (4) gives a corresponding structure of the mode $\xi(r)$. Substituting the mode structure into Eq. (3) to amend the eigenvalue of ω and repeating the procedure, we can finally determine the eigenvalue ω and the corresponding eigenfunction, i.e., the structure of the mode $\xi(r)$ together in the iterative process.

3. Numerical results

In order to explore the effects of a wide range of different q-profiles on the kink mode with energetic particles, especially when q_0 is greater than but close to unity, we present a series of the profiles in a simple model as $q = q_0\,(1+0.8(r/a)^{\alpha})^2$ as shown in Fig. 1. There are two parameters to control the shape of the profile, i.e., the safety factor at the magnetic axis, q_0, and the shear controlling parameter, α.

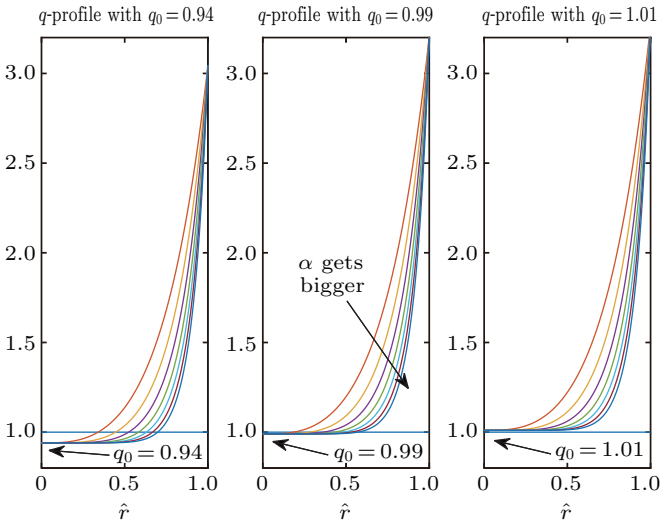


Fig. 1. (color online) Safety factor profile modeled by $q = q_0(1+0.8\hat{r}^{\alpha})^2$ with α increasing from 3 to 9.

We investigate the well-understood positive shear safety factor profile first, to validate our results. Then, we increase q_0 from 0.94 to 0.99 then 1.01, to investigate the non-resonant mode[26] regime of $q_0 > 1$ with no $q = 1$ rational surface existing. It is found that even if the mode is non-resonant due to the absence of $q = 1$ surface, it is still unstable due to energetic ions drive. Also for each fixed q_0, we change α from 3 to 9 to make the shear-free region of the q-profile wider and wider, thus we can clearly see that the boundary layer becomes more and more obscure, indicating spatial scale separation fails gradually.

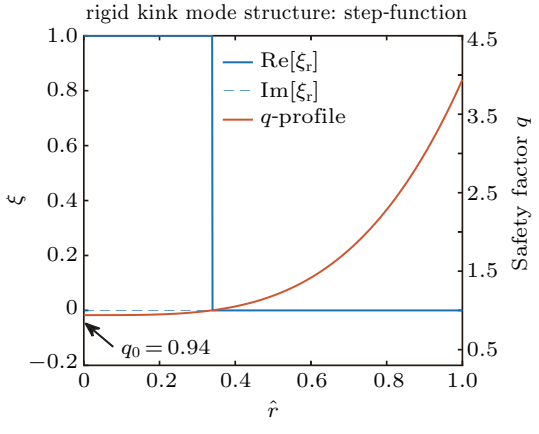


Fig. 2. (color online) Safety factor profile (red line), mode structure (solid blue line), and imaginary part of the mode structure (dotted blue line) which is zero under ideal-MHD condition.

First, we choose a positive finite magnetic shear profile with $q_0 = 0.94$, $\alpha = 3$, and no energetic ions. The result should be a rigid step-function for the conventional kink modes, as shown in Fig. 2. In ideal MHD, the mode frequency is then either purely real or purely imaginary and so is the mode structure,[27] and Alfvén continuum damping gives rise to a singular point where $k_{\|} = 0$, to induce a step function. With energetic ions, say $\hat{\beta}_{\rm h} = 0.05\%$, a real part of the frequency is introduced to the pure growth, and also an imaginary part is introduced to the pure real mode structure. Thus, the singular sheet with no width is resolved into a resonant layer as shown in Fig. 3. The real frequency of the mode is $\omega/\omega_{\rm A} = 0.005 + 0.0004\mathrm{i}$ which is about a half of precession frequency as predicted in Ref. [10].

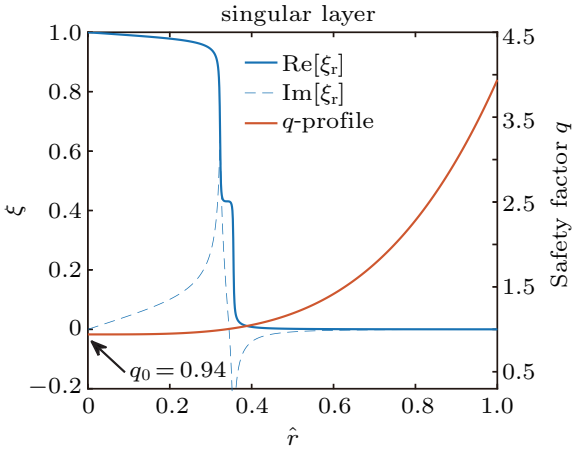


Fig. 3. (color online) Safety factor profile (red-line), real part (solid blue line), and imaginary part (dotted blue line) of the mode structure. Note that the imaginary part is non-zero.

Conventional fishbone mode requires several conditions: the rational surface, a finite discrepancy between q_0 and unity, a finite magnetic shear.[20] Due to the finite magnetic shear, the width of singular layer $\Delta/r_{\rm s} \sim \omega/\hat{s}\omega_{\rm A}$ with $\hat{s} = r_{\rm s}q'/q$ being very small compared with the minor radius because of $\omega/\omega_{\rm A} \sim O(\varepsilon^2)$. Scale separation can then still be done as in the conventional fishbone theory. Once the requirement is not satisfied, rigid step-function structure is not valid any more as indicated in Refs. [18] and [19]. Thus, results based on a step-function trial structure need to be revisited. We then investigate a low magnetic shear case and a case where there is no $q = 1$ rational surface to show it explicitly.

Figure 4(a) shows a low magnetic shear case with the shear control parameter $\alpha = 5$, $\hat{\beta}_{\rm h}$ is as low as 0.005%, and $q_0 = 0.99$. We find that even for such a low $\hat{\beta}_{\rm h}$, the mode structure shows a large deformation in comparison with that in the ideal MHD case in Fig. 4(b). That is to say, under a low magnetic shear, the step-function mode structure is not valid. Because of the low shear, Alfvén continuum damping

(represented by the peak of dotted line which is not so sharp as in Fig. 3) becomes weak, thus a low energetic ion drive can be enough to cause an instability. And due to the low magnetic shear, the singular layer $\Delta \sim \hat{s}^{-1}$ is widened, and the scale separation is not clear, which means that the singular layer disappears and the mode becomes more like infernal mode structure.[19] Though the mode is still internal, the slop of the mode structure suggests that the fluctuation energy will be concentrated in a smaller core region, causing the level of saturation of the fluctuation in core to be higher than that in the MHD case.

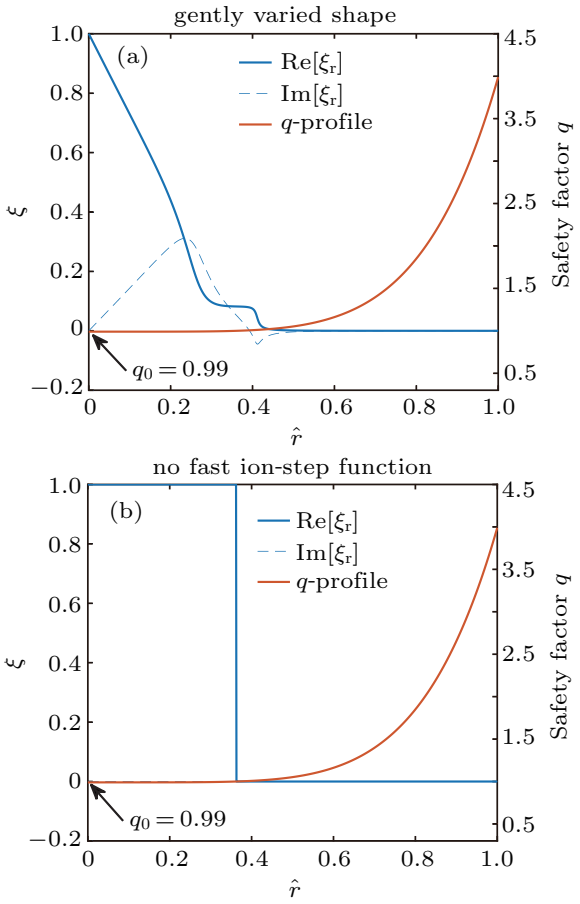


Fig. 4. (color online) Low magnetic shear case with $q_0 = 0.99$ and $\alpha = 5$ with (upper)/without (lower) energetic ions. The red line represents the q-profile and the blue line denotes the mode structure.

In order to further understand the competition between the stabilization factor, α (related to the shear), and destabilization factor, $\hat{\beta}_h$, we perform a parameter scan in α–$\hat{\beta}_h$ space with fixed q_0= 0.99 as shown in Fig. 5 with the contour plot for the mode growth rate. We can see that the growth rate depends much more strongly on $\hat{\beta}_h$ than α. The parameter α determines the width of the shear-free region of the q-profile as shown in Fig. 1 evidently. As α increases, the shear-free region expands, and so does the unstable region. And thus, the growth rate of the mode is faster.

When q_0 is slightly greater than unity, the $m/n = 1/1$ mode should be stabilized in the pure MHD regime. Nevertheless, due to the weak shear, the pressure driven term becomes marginally unstable, which is however a fourth order contribution to a very slowly growing mode. On the other hand, the low magnetic shear corresponds to weak Alfvén continuum damping. Then with energetic ions injected to the plasma, the strong gradient of the fast ion pressure will release free energy to overcome the damping, to dirve an instability. So, in our numerical procedure, we exclude the plasma pressure contribution, but retain the energetic particles contribution. Due to the fact that the low magnetic shear weakens the damping mechanism, the mode structure can stretch within a wide region and even a small drive can cause a fast-growing instability.

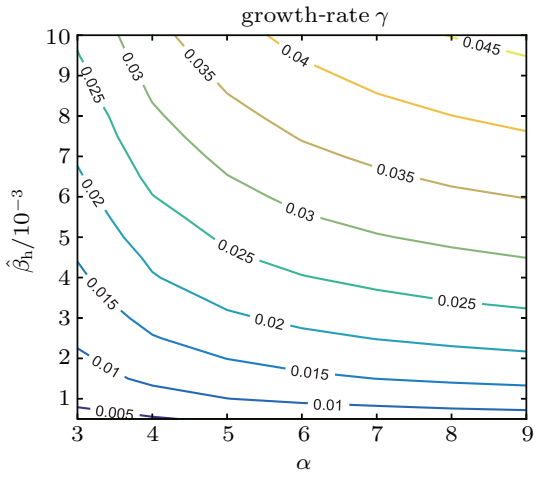


Fig. 5. (color online) Mode growth-rate γ dependence on α and $\hat{\beta}_h$ with fixed $q_0 = 0.99$. The solid line represents the contour line of γ, which increases from lower left to upper right.

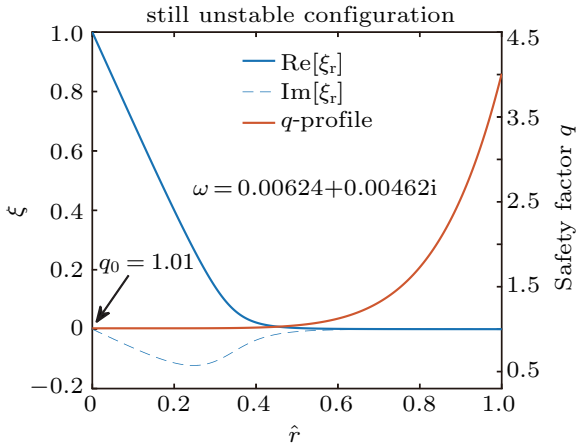


Fig. 6. (color online) Mode structure when q_0 is slightly greater than unity and high-energy particle beta $\hat{\beta}_h = 0.05\%$, with the red-line for the safety factor profile, the solid blue line for the real part, and the dotted blue line for the imaginary part of the mode structure.

Figure 6 shows such a case with $q_0 = 1.01$ and $\hat{\beta}_h = 0.05\%$. There is a peak in the imaginary part of the mode structure, corresponding to the minimum $k_\parallel$, but Alfvén resonance. Its growth rate is then comparable to the mode frequency. Such a fast-growing instability may degrade the confinement dramatically.

To further understand the difference between core safety factor greater than unity and core safety factor lower than unity, we perform the same parameter scan as did above, and the results are shown in Fig. 7. When the low shear region widens, the unstable region becomes larger, and the growth rate of the mode rises up because of weaker damping mechanism. And with increasing $\hat{\beta}_h$, the growth-rate ramps up just as expected, which proves strongly that the instability is also driven by energetic particles. One may note that there is not a significant difference between Fig. 5 and Fig. 7, thus showing the most interesting fact that no matter whether the $q = 1$ rational surface exists the 1/1 internal mode stability is not affected, if q_0 is constrained in the vicinity of unity, which is very different from the scenario of ideal MHD due to the energetic particle drive.

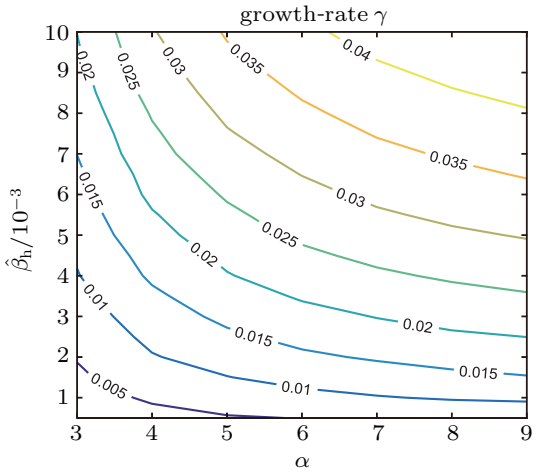


Fig. 7. (color online) Distributions of the mode growth-rate γ in the (α, $\hat{\beta}_h$) space with $q_0 = 1.01$.

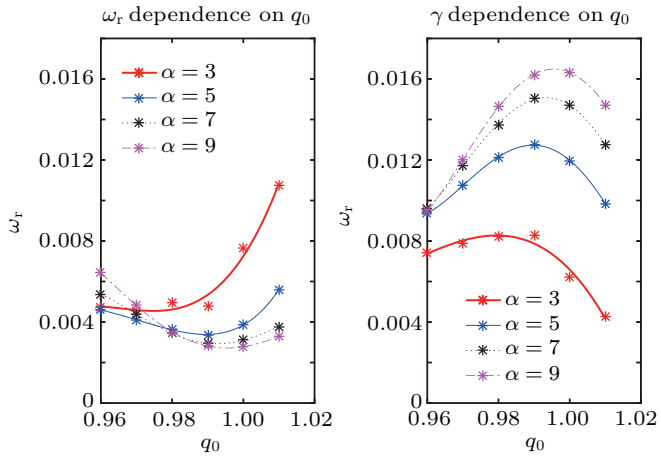


Fig. 8. (color online) Dependence of the mode frequency and growth-rate on the central safety-factor q_0 with $\beta_h = 0.15\%$, and α is changed from 3 to 9. Stars are calculated results, and the lines are fittings to them.

This results can be deduced explicitly from Fig. 8, which shows the dependence of mode frequency and growth-rate on central safety-factor $q_0 = q(r = 0)$ with $\beta_h = 0.15\%$. The stars in the figure are obtained by our numerical procedure, while the lines are fittings, for four different shears. The frequency of the mode decreases with q_0 when it is obviously below unity, i.e., in the resonant mode case, but rises up in the $q_0 > 1$ regime, i.e., in the non-resonant mode case, after a transition regime for $q_0 \lesssim 1$. And the growth-rate of the modes shows a similar transition property of rising in the significant $q_0 < 1$ regime and dropping in the $q_0 > 1$ regime, with the transition in the region of $q_0 \lesssim 1$. This is because the mode is excited by interaction of EPs with $m/n = 1/1$ internal kink mode, as q_0 increases to the regime above unity, the resonance surface is lost and the growth-rate of the non-resonant mode drops down. Also, the shear decreases as the parameter α increases, so that the growth rate of the mode rises.

4. Conclusions

Unlike previous work on fast ion driven kink modes, we consider the special q-profiles with a wide shear-free region, so that the spatial scale separation fails. And a self-consistent method is then used to recalculate the linear instability in such tokamak plasmas. A general dispersion relation and a mode structure equation are used to determine the eigenmode structure and eigenvalue frequency simultaneously. By studying various q-profiles, we find that the weaker the magnetic shear, the more similar the mode structure is to that of infernal mode with a feature of gently varied shape instead of the rigid kink mode structure. Even when q_0 is greater than unity, i.e., the resonance is removed, energetic particles can drive a non-resonant instability, whose unstable region can stretch across a wide region and whose growth rate is comparable to its real frequency. And thus, rational surface is not an important factor in determining the properties of the instability when energetic particles are present in plasma.

Acknowledgment

The author Wen-Ming Chen would like to thank Dr. Guo Meng for helpful discussion.

References

[1] Van Dam J W 2009 *Plasma and Fusion Research* **4** 035
[2] Rosentbluth M N and Rutherford P H 1975 *Phys. Rev. Lett.* **34** 1428
[3] Tsang K T, Sigamr D J and Whitson J C 1981 *Phys. Fluids* **24** 1508
[4] Fasoli A, Gormenzano C, Berk H L, Breizman B, Briguglio S, Darrow D S, Gorelenkov N, Heidbrink W W, Jaun A, Konovalov S V, Nazikian R, Noterdaeme J M, Sharapov S, Shinohara K, Testa D, Tobita K, Todo Y, Vlad G and Zonca F 2007 *Nucl. Fusion* **47** S264
[5] Weiland J, Lisak M and Wihelmsson H 1987 *Phys. Scr.* **T16** 53
[6] Fu G Y and Van Dam J W 1989 *Phys. Fluids B* **1** 1949
[7] Chen L 1994 *Phys. Plasma* **1** 1519
[8] Gorelenkov N N, Pinches S D and Toi K 2014 *Nucl. Fusion* **54** 125001
[9] McGuire K, Goldston R, Bll M, Bitter M, Bol K, Brau K, Buchenauer D, Crowley T, Davis S and Dylla F 1983 *Phys. Rev. Lett.* **50** 891
[10] Chen L, White R B and Rosenbluth M N 1984 *Phys. Rev. Lett.* **52** 1122

[11] White R B, Chen L, Romanelli F and Hay R 1985 *Phys. Fluids* **28** 278
[12] Coppi B and Porcelli F 1986 *Phys. Rev. Lett.* **57** 2272
[13] Wu Y L, Cheng C Z and White R B 1994 *Phys. Plasmas* **1** 3369
[14] Chen W, Ding X T, Liu Y, Yuan G L, Zhang Y P, Dong Y B, Song X Y, Zhou J, Song X M, Deng W and Yang Q W 2008 *Chin. Phys. Lett.* **25** 3708
[15] Xu L Q, Hu L Q and EAST team 2013 *Chin. Phys. Lett.* **30** 075201
[16] Chen W, Ding X T, Liu Yi, Yang Q W, Ji X Q, Isobe M, Yuan G L, Zhang Y P, Zhou Y, Song X Y, Dong Y B, Li W, Zhou J, Lei G J, Cao J Y, Deng W, Song X M, Duan X R and HL-2A Team 2010 *Nucl. Fusion* **50** 084008
[17] Rosenbluth M N, Dagazian R Y and Rutherford P H 1973 *Phys. Fluids* **16** 1894
[18] Crew G B and Ramos J J 1983 *Phys. Fluids* **26** 2621
[19] Zhang R B, Wang X Q, Xiao C J, Wang X G, Liu Y, Deng W, Chen W, Ding X T, Duan X R and HL-2A Team 2014 *Plasma Phys. Control. Fusion* **56** 095007
[20] Hastie R J, Hender T C, Carreras B A, Charlton L A and Holmes J A 1987 *Phys. Fluids* **30** 1756
[21] Meng G, Wang X Q, Wang X G and Zhang R B 2015 *Phys. Plasmas* **22** 092510
[22] He H D, Dong J Q, Fu G Y, He Z X, Jiang H B, Wang Z T, Zheng G Y, Liu F, Long Y X, Shen Y and Wang L F 2011 *Nucl. Fusion* **51** 113012
[23] Bussac M N, Pellat R, Edery D and Soule J L 1975 *Phys. Rev. Lett.* **35** 1638
[24] Candy J, Berk H L, Breizman B N and Porcelli F 1999 *Phys. Plasmas* **6** 1822
[25] Zhang Y Z, Berk H L and Mahajan S M 1989 *Nucl. Fusion* **29** 848
[26] Yu L M, Chen W, Jiang M, Shi Z B, Ji X Q, Ding X T, Li Y G, Ma R R, Shi P W, Song S D, Yuan B S, Zhou Y, Ma R, Song X M, Dong J Q, Xu M, Liu Y, Yan L W, Yang Q W, Xu Y H, Duan X R and HL-2A Team 2017 *Nucl. Fusion* **57** 036023
[27] Wesson J A 1978 *Nucl. Fusion* **18** 87